Synthesis and Structural Analysis of Magnesium Oxide Nanomaterial Using Ethanol as Polymerization Solvent

I Wayan Sutapa[1]*, Abdul Wahid Wahab[2], Paulina Taba[2], Nursiah La Nafie[2]

[1]Department of Chemistry, Faculty of Mathematics and Natural Science, Pattimura University, Jalan Ir. Putuhena No. 1 Ambon Maluku.

[2]Department of Chemistry, Faculty of Mathematics and Natural Science, Hasanuddin University, Jalan Perintis Kemerdekaan Km 10, Makassar-Indonesia

*Corresponding Author: wayansutapa@fmipa.unpatti.ac.id

Abstract

The purpose of the study was to synthesize MgO nanomaterials using sol-gel method with ethanol as solvent and to perform structural analysis of the products. Mg-oxalate was initially prepared prior magnesium acetate. Magnesium acetate dissolved in ethanol, and the oxalic acid added to adjust pH until gel phase formed. The gel was heated at 100 °C for 24 hours to produce magnesium oxalate solids. Solids was sieved using ±150 mesh then annealed at 550 °C for 6 hours to produce MgO nanomaterial. The magnesium oxalate was characterized using FT-IR, XRD, and SEM. FT-IR peak at 3408.22 cm^{-1}; 1709.35 cm^{-1}; 1375.39 cm^{-1}; 830.32 cm^{-1}; 420.48 cm^{-1}, and the XRD peak 17.95°; 22.97°; 25.02°; 27,94°; 35.10°; 37,63°; 44.16° were characteristic of Mg-oxalate. Meanwhile, FT-IR band at 1030.24 cm^{-1}; 2358.94 cm^{-1}; 1627.92 cm^{-1}; 1417.66 cm^{-1}; 437.84 cm^{-1}, and XRD peak at 38.92°; 43.3°; 56.02°; 62.64°; 74.88° and 79.04° shows characteristic of MgO nanomaterial. Structure analysis shown the MgO nanomaterials has an average crystal size 8.11 nm, and lattice length 21.21 nm. The values of strain, stress, energy density crystal and dislocation density of the MgO are 5.3 x 10^{-5} MPa, 32.97 MPa, 154.81 J/nm^2, 1.52 x 10^{-3} nm^{-2} respectively. Morphologically the MgO nanomaterial produced is cubic.

Keywords: Nanomaterial, MgO, sol-gel, strain, stress, energy density, dislocation density.

Abstrak (Indonesian)

Penelitian ini bertujuan mensinstesis nanomaterial MgO menggunakan metode sol-gel menggunakan etanol sebagai pensolvasi serta analisis struktural terhadap produk yang dihasilkan. Mula-mula Mg-oksalat dipreparasi sebagai prekursor dari magnesium asetat. Magnesium asetat disolvasi dalam etanol dan pH larutan yang diatur hingga 5. Gel yang terbentuk dipanaskan pada suhu 100 °C selama 24 jam. Padatan dihaluskan ±150 mesh kemudian di*anealing* pada suhu 550 °C selama 6 jam. Produk yang diperoleh dikarakterisasi menggunakan FT-IR, XRD dan SEM. Hasil FT-IR pada 3408,22 cm^{-1}; 1709,35 cm^{-1}; 1375,39 cm^{-1}; 830,32 cm^{-1}; 420,48 cm^{-1}, dan hasil XRD pada peak 17,95°; 22.97°; 25,02°; 27,94°; 35,10°; 37,63°; 44,16° adalah karakteristik Mg-oksalat. Nanomaterial MgO dikarakterisasi dengan FT-IR pada pita 1030,24 cm^{-1} 2358,94 cm^{-1} 1627,92 cm^{-1} 1417,66 cm^{-1}, 437.84 cm^{-1} dengan hasil uji XRD pada peak 38,92°; 43,3°; 56,02°; 62,64°; 74,88° and 79,04°. Nanomaterial MgO memiliki ukuran kristal rata-rata 8,11 nm dan panjang kisi rata-rata 21,21 nm. Nilai *strain, stress*, kerapatan energi, dan kerapatan dilokasi namomaterial MgO berturut-turut adalah 5,3 x 10^{-5} MPa, 32,97 MPa, 154,81 J/nm^2, 1,52 x 10^{-3} nm^{-2}. Secara morfologi nanomaterial MgO yang dihasilkan berbentuk kubik.

Kata kunci: Nanomaterial, MgO, sol-gel, strain, stress, kerapatan energi, kerapatan dislokasi.

INTRODUCTION

Metal oxides with nano-sizes in recent years have attracted many researchers. This condition is due to a metal oxide material has unique properties different from bulk material. One of these nanomaterials is MgO. MgO nanomaterial is a material that has quite a lot of applications, including as additional material for the manufacture of ceramics

[1], paint additives [2], superconductors [3], catalysts [4] and catalyst carriers [5], absorbing toxic waste materials in waters [6], and gas adsorbents [7]. Other applications as layers to grow thin film materials,there are the widely used other advantages of MgO nanomaterials which have large bandgap and high-temperature stability [8].

MgO nanomaterials produced through the decomposition process of magnesium or magnesium hydroxide salts are a commonly used method [9]. The nanomaterial produced by this method has a small surface area and a large particle size. These two characters of nanomaterial products can reduce the ability of MgO to be applied to a wider field. Therefore, many synthesis methods have been developed to obtain nanomaterials that can be applied in various fields. Synthesis of sol-gel method [10,11], hydrothermal application [12], precipitation method [13], combustion path [14], sonication method [15], decomposition method [16], and surfactant application method [17] are methods used to produce MgO nanomaterials today.

The sol-gel method using magnesium acetate dissolved in ethanol to produce Mg-oxalate as a precursor. This method is the most widely used insucmuch as the synthesis process with this method is more straightforward, not require advanced equipment, and the material used is relatively cheaper [18]. The morphology, crystal size, and specific surface area of the MgO nanomaterials produced can be arranged using this synthesis method. However, the structural analysis of the MgO nanomaterials produced to date is a challenge in itself. The method conducted due to understanding the structural characteristics of the nanomaterials produced, will be helpful to know the development of appropriate advanced applications for this material.

The literature study conducted shows that there have been no reports of structural analysis of MgO nanomaterials produced using ethanol solvents in the formation of Mg-oxalate as precursors. Based on this background, this study carried out the synthesis of MgO nanomaterials using ethanol solvents through the Mg-oxalate reaction pathway as a precursor. The synthesized product was analyzed using FT-IR, XRD, SEM, and structural analysis.

MATERIALS AND METHODS

Materials

The materials used in this study were $C_2H_4 \cdot 2H_2O$ (Sigma Aldrich), $Mg(CH_3COO)_2 \cdot 4H_2O$ (Sigma Aldrich), Whatman-40 filter paper, filter paper, ethanol (Merck), distilled water, bi-distillet water.

Methods

MgO nanomaterials were synthesized using the sol-gel method to produce Mg-oxalate as a precursor followed by annealing. Magnesium acetate tetrahydrate 30 grams is dissolved in ethanol until the solution is transparent. The pH of the mixture adjusted by adding 1 M oxalic acid little by a little while stirring until the whitening gel produced. The gel obtained is left overnight for the deposition process. The Mg-oxalate obtained was dried at 100 °C for 24 hours, smoothed and sifted with a ± 150 mesh sieve and analyzed by FT-IR, SEM-EDX, and XRD.

Furthermore, the annealing process was carried out at a temperature of 550 °C for 6 hours. The resulting MgO nanomaterials were characterized using FT-IR, XRD, and SEM. Then, the MgO nanomaterial analyzedof the crystal structure.

RESULTS AND DISCUSSION

Synthesis of MgO Nanomaterial Precursors

MgO nanocatalyst synthesis in this study was carried out using the sol-gel method. The production of MgO nanocatalyst was initiated by synthesizing Mg-oxalate as precursors from $Mg(COOH)_2 \cdot 4H_2O$ and $C_2H_2O_4$ magnesium acetate.

Magnesium tetrahydrate is initially dissolved using absolute ethanol to produce a mixture of magnesium (Mg^{2+}) and acetate ($-COO^-$) ions. The mixture added 1 M oxalic acid slowly until the pH of the mixture reaches 5. The addition of oxalic acid to reach this pH aims to form a complex and polymerize magnesium with oxalate ions simultaneously. Complex formation and polymerization of magnesium and oxalate characterized by changes in the mixture of sols to white gel as shown in Figure 1.

In addition to producing magnesium oxalate complexes, polymerization and complexation reactions also form by-products namely acetic acid and water. The resulting side products removed through a drying process at a temperature of 100 °C for 24 hours. The by-products produced will evaporate as indicated by the loss of the smell of acetic acid from the product and the reduction in product weight by 5%. The results of magnesium oxalate characterization before and after heating were carried out using FT-IR, XRD and SEM instruments. The formation of MgO nanomaterials is carried out through a complexation reaction pathway to form Mg-Oxalate precursors.The polymerization process to

form linear polymer networks and calcination processes for the formation of MgO nanomaterials [19].

The synthesis of the Mg-oxalate precursor preceded by the formation of Mg^{2+} ions using $Mg(CH_3COO)_2 \cdot 4H_2O$ in ethanol solvents. The prediction of the dissolved Mg^{2+} ion in ethanol shown in Figure 2. Ethanol was chosen as a solvent with consideration because it has a large total energy of -14382.44 kcal/mol.


(a)   (b)

Figure 1. Formation of Mg-oxalate

The energy possessed by ethanol is enough to break the $Mg-CH_3COOH$ bond which has a binding energy of -1529.77 kcal/mol without the need for additional heating. In addition, ethanol selection of ethanol as a solvent also functions as a solvent for Mg^{2+} ions to remain stable in ionic conditions.
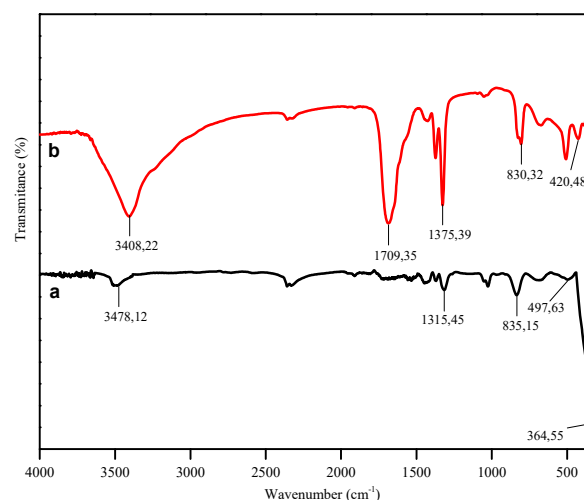
Characterization of Magnesium Oxalate using FT-IR

The results of the analysis with FTIR on magnesium oxalate before and after heating shown in Figure 14 (a-b). The tape that appears at 3478 cm^{-1} and 3408.22 cm^{-1} generated from the vibrational group (-O-H) which forms hydrogen bonds derived from acetic acid. Strain vibration of (–COOH) (dimer) shown at 1315 cm^{-1}. The 835.15 cm^{-1} band produced by strain vibration (-C-O-C-). The vibration produced by Mg-O appears in the band 497.63 cm^{-1} and the vibration of the bond strain (-C-O-) is shown in the band 364.55 cm^{-1}. Figure 14 (b) shows the presence of a band produced by an overtone strain vibration (-C=O).

The sharp bands 1709.35 cm^{-1} and 1375.39 cm^{-1} derived from the vibrational strain of -C-O asymmetry in the Mg-oxalate complex. Strain vibration originating from (-C-O-C-) appears in the band 830.32 cm^{-1} and the Mg-O vibration indicated by the presence of a medium band at 420.48 cm^{-1} [20].
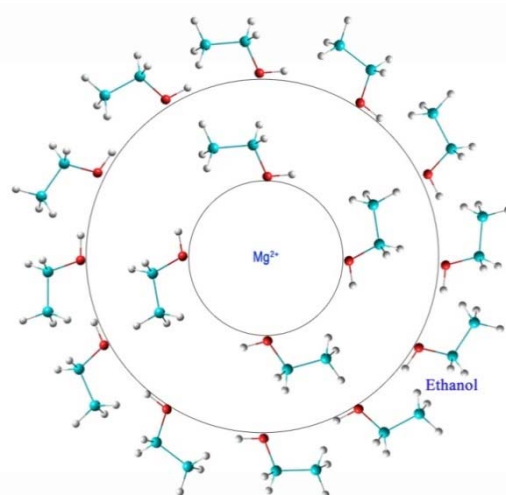
Figure 2. Solvation of Mg^{2+} ions by ethanol (two-layer system)

Figure 3. Spectrum FT-IR of magnesium oxalate (a) before (b) after heating

Characterization of Magnesium Oxalate using XRD

The results of XRD analysis on magnesium oxalate before and after heating are shown in Figure 4. These results show no significant difference in Mg-oxalate before and after heating, this is because the polymer structure does not change during heating 100°C. It appears that Mg-oxalate has been formed before heating and undergoes refinement after heating which is indicated by reduced impurity peak as shown in Figure 4 (b).Peaks at 2θ: 17.95°; 22.97°; 25.02°; 27,94°; 35.10°; 37,63°; 44.16° with miller indexes (110), (202), (213), (212), (213), (022), (023) which are the hallmarks of magnesium oxalate [21,22].

Synthesis of MgO Nanomaterial

The synthesized product of MgO nanomaterials was characterized using FT-IR, XRD, and SEM. This characterization aims to ensure the nanomaterial products produced in accordance with MgO characters in general.
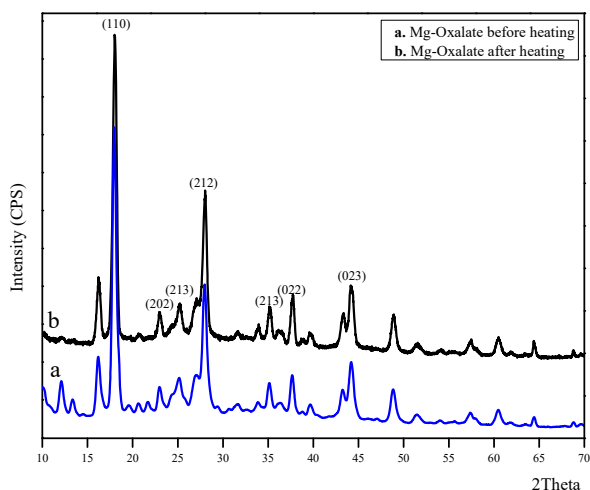

Figure 4. Diffractogram of magnesium oxalate

Characterization of MgO Nanoparticles with FT-IR

Analysis of functional groups of MgO nanoparticles using FT-IR with a scan of 350 cm^{-1} to 4000 cm^{-1}. The presence of a band that appears at wave number 3697.47 cm^{-1}, reinforced with a band that appears at 1030.24 cm^{-1} showing the vibration of the -OH strain derived from water absorbed on the surface of the MgO molecule. The band at 2358.94 cm^{-1} originates from the vibration stretching of CO_2.

Another band that appeared at 1627.92 cm^{-1} produced from the interlayer deformation process of H_2O molecules. The absorption that appears in the band 1417.66 cm^{-1} shows a strain of Mg-O that binds H from water. Streching vibration produced by the Mg-O-Mg bond appears on the band with wave number 437.84 cm^{-1} as a broad-band. Analysis of all bands that appear in Figure 5 shown in Table 1.

Analysis MgO Nanomaterial using XRD

The XRD diffractogram pattern of MgO nanoparticles produced from the annealing process at a temperature of 550ºC shown in Figure 6. The peaks of the MgO nanoparticles compared to the standard MgO (JCPDS No.75-1525) to ensure purity. There are peaks that appear at angles 2θ: 38.92º, 43.3º, 56.02º, 62.64º, 74.88º and 79.04º with the Miller index (111), (200), (220), (220), (311), and (222) are characteristics of MgO nanoparticles.
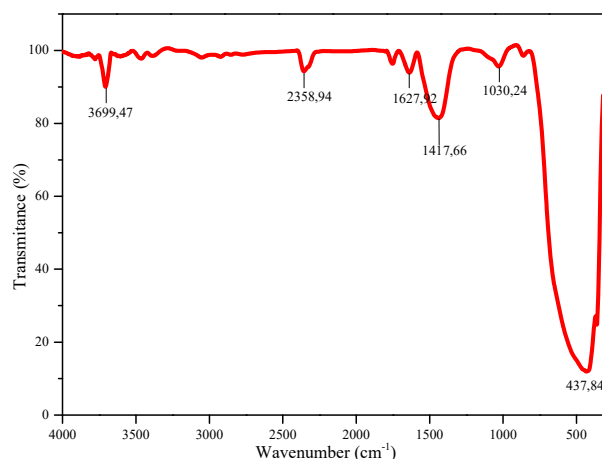

Figure 5. A spectrum of FT-IR MgO nanoparticles

Table 1. Spectrum of FT-IR MgO nanomaterials

Vibration Mode	Wavenumber (cm^{-1})
Vibration stretching H-O-H from the water on the surface	3699.47
Vibration stretching CO_2	2358.94
Deformation vibration *interlayer* H_2O	1641.92
MgO vibration binds H from H_2O	1417.66
Vibration stretching -Mg-O-Mg-	437.84

Furthermore, based on the peaks that are characteristic of MgO nanoparticles, the average crystal size (D) and lattice length (a) are determined.

The determination of the crystal size of the average MgO was carried out using the Debye-Scherer equation [23].

$$D = \frac{K\lambda}{\beta cos\theta} \qquad (1)$$

Where *D* the average crystal size, K is the Debye-Scherer constant (0.94), λ is the CuKα radiation wavelength (0.154 nm), *β* is the full width half maximum (FWHM) of the peak, θ is the diffraction angle of MgO nanoparticles.

Lattice length of each peak determined using the extending of Bragg's law:

$$2d\,Sin\,\theta = n\,\lambda \qquad (2)$$
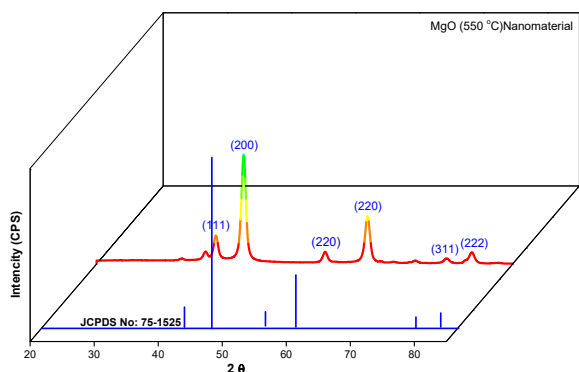
For cubic crystals form applied the equation:

Figure 6. Diffractogram of MgO nanomaterials

$$\frac{1}{d^2} = \frac{h^2+k^2+l^2}{a^2} \qquad (3)$$

The substitution of equation 2 into equation 3 will produce equation 4 as follows:

$$a = \frac{\lambda}{2\sin\theta} \; x \; \sqrt{h^2+k^2+l^2} \qquad (4)$$

Where a is the crystal lattice length, *h k l* is the Miller crystal index, d is interplanar distance between atoms, λ is the CuKα radiation wavelength (0.154 nm), θ is the diffraction angle of MgO nanoparticles. The results of the calculation of crystal size and lattice length for each temperature variation of the MgO formation annealing shown in Table 1.

The size of MgO nanomaterial crystals obtained an average of 8.11 nanometers. This result is higher than MgO nanomaterials which are synthesized using methanol solvents to dissolve magnesium acetate [24].

Table 2. Results of calculation on crystal size and lattice length of MgO

2θ (°)	FWHM	h k l	Particle size (nm)	Lattice parameter (nm)
38.57	0.553	(111)	9.52	16.49
42.91	0.504	(200)	9.16	18.32
55.62	0.556	(220)	8.62	24.39
62.23	0.526	(220)	7.86	22.25
74.58	0.519	(311)	6.84	22.69
78.49	0.532	(222)	6.68	23.14
	Average		**8.11**	**21.21**

Application methanolat previous studies as a solvent for Mg^{2+} can reduce the size of the nanomaterial produced. It is due to the lack of steric disturbances possessed by the methanol-Mg^{2+} complex compared to the ethanol-Mg^{2+} complex. The results of calculating the lattice parameters possessed by MgO nanomaterials show the lattice parameter average of 21.21 nm. Average values of these lattice parameters obtained are smaller than the parameters of the MgO nanomaterial lattice based on JCPDS no. 76-1525 (a = 4.21 Å) [25].

Analysis of the Size Distribution of Nanomaterial MgO

The pattern of the distribution of the size of the nanomaterial crystals can be known through the crystal size distribution. Crystal size distribution is analysed using a model that assumes that the crystals formed are considered to be distributed logarithm normally [11]. Based on the reference model, the formulation of the MgO nanomaterial size distribution described in equation 5.

$$DF_{MgO} = T \; exp\left[-\frac{[ln(D/m_{MgO})]^2}{2\sigma^2}\right] \qquad (5)$$

Where DF is the size distribution of the MgO nanomaterial, D is the size of the nanomaterial every angle, σ is the value of the variant produced, $T = \frac{1}{\sqrt{2\pi}\sigma_{MgO}}\frac{1}{x}$, and m_{MgO} is the median value of the size of the nanomaterial. Based on the results of calculations using the results of calculations using functions in equation 5 produce a graph of particle size distribution in Figure 7.

Figure 7 shows that MgO nanomaterials synthesized have a distribution of most crystallite sizes of less than 10 nm with variants of 1.41 and median 8.24. The size of the MgO nanomaterial produced is less than 10 nm which indicates that this synthesis method is successfull in synthesizing MgO entirely [24].
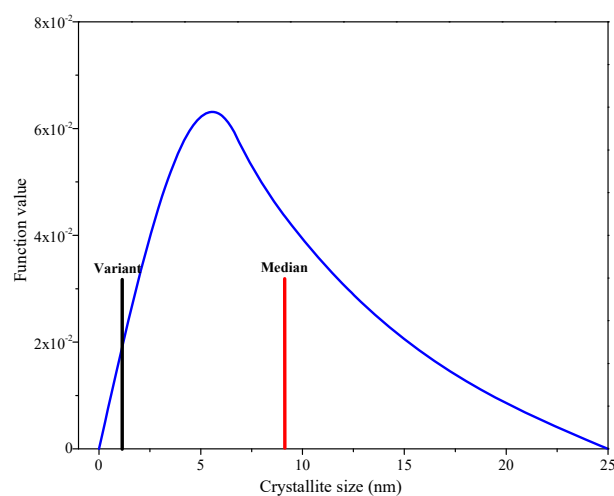

Figure 7. MgO nanomaterial size distribution

Analysis of Strains of MgO Nanomaterials

Nanomaterial strains play a significant role in determining the characteristics and properties of the nanomaterials produced. Nanomaterial strains are an increase in the size of the crystals caused by changes in temperature treatment, bond forms and Van Der Waals bonds given at the time of nanomaterial formation. The magnitude of the strain value possessed by nanomaterials can be determined using the assumption that all the area around the crystal is isotropic, and the nanomaterial crystals that exist are not interdependent in all directions and have uniform shapes in all directions [26]. Based on these assumptions, the crystal strain can be determined using a uniform deformation model as in equation 6.

$$R \cos \theta = T + 4\,c \sin \theta \qquad (6)$$

Where R is FWHM MgO nanomaterials are calculated using equations; $R = \left[(T^2)_{sampel} - (T^2)_{stand.}\right]^{1/2}$, θ is the diffraction angle of X-RD, T=(K x 0,1541)/D and c is a MgO nanomaterial strain. Plot 4 sin θ versus R cos θ from equation 6 shown in graph Figure 8.


Figure 8. Plot of 4 Sin θ vs R cos θ
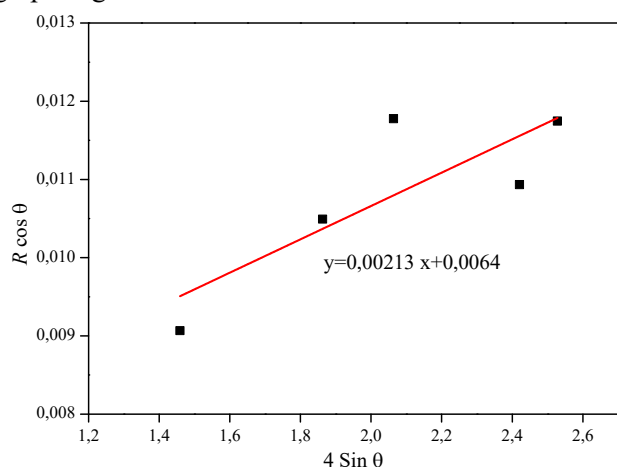
Based on the value of the slope obtained 0.00213 and the intercept value obtained at 0.0064. Referring to the plot in Figure 8, the strain value (c) obtained 5.3 x 10^{-5} MPa. The results of the low strain calculation indicate that the MgO nanomaterial produced using the sol-gel method has a crystal structure which changes the crystal structure very little. This condition caused by the repulsion of Van Der Waals between atoms making up small nanomaterials so that the rearrangement of bonds between atoms tends not occurred [27].

Stress Calculation of MgO Nanomaterials

The stress value analysis of a nanomaterial is an attempt to understand the strength of the nanomaterial crystals to respond to the pressure applied. The magnitude of the different ability of the crystals of the nanomaterial to respond to pressure is caused by differences in crystal arrangement imperfections. The equation used to determine the value of stress is a modification of Williamson-Hall. The results of this equation modification based on the assumption that the crystal structure to be tested has a uniform shape. In addition, if the Hook Law is applied, the strain value and stress are linear [28]. Based on these assumptions, the modifications to determine stress values shown in equation 7.

$$R \cos \theta = T + 4\,t \sin \theta / L \qquad (7)$$

Where t is the stress value of the crystalline value of the nanomaterial, L is the constant modulus young MgO (248.7 GPa at 293 K), R is the value of FWHM. The value of equation 7 obtained then plotted 4 sinθ/L versus R cos θ shown in Figure 9.


Figure 9. Plot of 4 Sin θ/L vs R cos θ
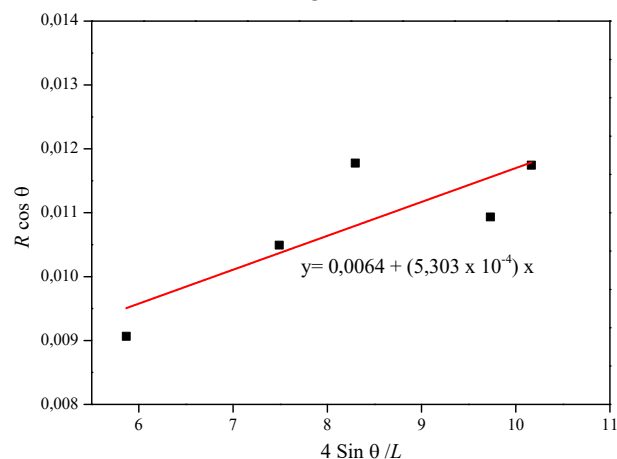
The linear regression results obtained by intercept are 5.303 x 10^{-4} MPa. Based on the value of the intercept can be calculated that the stress value of MgO nanomaterials produced is 32.97 MPa. This stress value indicates that the MgO nanomaterials produced can respond to a considerable pressure before changing the crystal structure [28].

The Estimated Crystalline Energy Density of MgO Nanomaterials

The assumption that the nanomaterials are homogeneous and isotropic can be used to determine the crystal density of nanomaterials. Based on these assumptions, equation 8 can used for to determine the nanomaterial crystal energy.

$$R \cos \theta = \mathrm{T} + \left[4 \sin \theta \sqrt{\frac{2E_d}{L}} \right] \quad (8)$$

The results of the calculation of equation 6 are then plotted, resulting in a graph in Figure 10. Based on the regression of the liner applied in Figure 10, the slope value of 4.29×10^{-4}. The slope value used to calculate the density energy possessed by MgO nanomaterials, the value of the MgO nanomaterial crystal energy density is 154.81 J/nm^2.
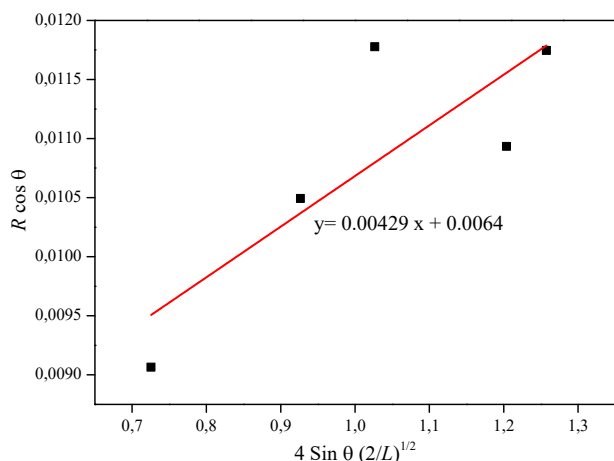
Figure 10. Plot of $4 \sin \theta (2/L)^{1/2}$ vs $R \cos \theta$

The energy of the crystal density of MgO nanomaterials is more significant than in the bulk form. The differences caused the crystal size MgO resulted in this process is on the nanoscale. The nanomaterial will have different characteristics from the micro size, and the macro [29].

The Dislocation Density of MgO Nanomaterials

Nanomaterial crystals can experience dislocation through the process of initiation, nucleation, or dispersion. Density dislocation of a material is one way to find out the level of defects possessed by crystals or deviations in the form of crystals that make up solid material. Usually, the dislocation density will decrease with increasing temperature of nanomaterial formation because an increase in temperature can reduce the number of imperfect crystals in the nanomaterial. In addition, the hardness of the crystals will increase along with the reduction in the value of material dislocation density [30]

The dislocation density of MgO nanomaterials produced in this study was determined using equation 7 [31].

$$\delta_{mat} = 1/D^2 \quad (7)$$

Where δ_{mat} is location density, D is the average value of MgO nanomaterial crystal size. Based on the calculation results, the dislocation density of MgO nanomaterials produced from the sol-gel process and followed by the heating method is 1.52×10^{-3} nm^{-2}. This result gives a hint that the value of the dislocation density of MgO nanomaterials produced is small. Density Dislocation of the resulting MgO nanomaterials can give an idea that the nanomaterials produced have small defective impurities or crystals. This is due to the high synthesis temperature of MgO nanomaterials can provide an opportunity for MgO crystals to undergo rearrangement. High temperatures can also prevent large numbers of defective crystals forming [30].

Morphological Analysis of MgO Nanomaterials

Morphological analysis using SEM and on MgO nanomaterials is shown in Figure 10.

(a)

(b)
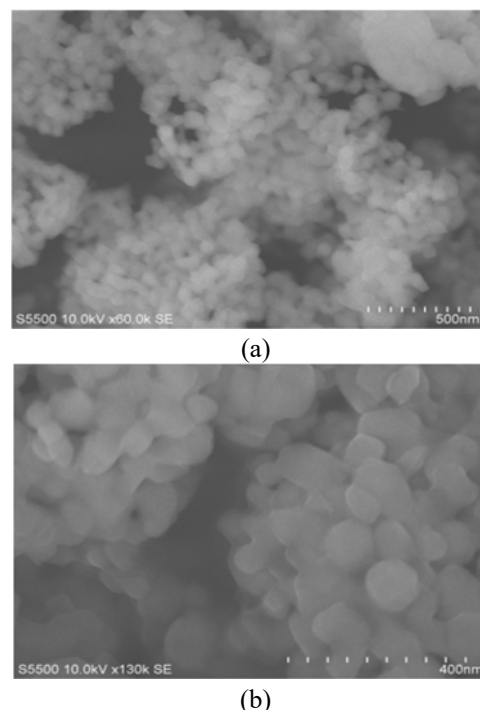
Figure 11. SEM analysis results

The results of the morphological analysis using SEM and on MgO nanomaterial showed that the resulting MgO nanocatalysts formed correctly. SEM results showed that the particle size obtained is not uniform, but the size still on the nanoscale range (less than 100 nm).

CONCLUSION

Based on the results of studies that have conducted, it was found that MgO nanomaterials can be synthesized using the sol-gel method with ethanol as solvents, through the Mg-oxalate pathway.

Characterisation using FT-IR, XRD, SEM, and structural analysis showed that the MgO nanomaterials obtained had distinctive characteristics as nanoscale-sized materials differing compared to the bulk material.

REFERENCES

[1] J.-F. Lang, J.-G. You, X.-F. Zhang, X.-D. Luo, and S.-Y. Zheng, "Effect of MgO on thermal shock resistance of CaZrO$_3$ ceramic," *Ceramics Intern.*, vol. 44, no. 18, pp. 22176–22180, Dec. 2018.

[2] F. Karakaş, G. Pyrgiotakis, M. S. Çelik, and B. M. Moudgil, "Na-Bentonite and MgO Mixture as a Thickening Agent for Water-Based Paints," *KONA Pow. Part. J.*, vol. 29, pp. 96–106, 2011.

[3] N. S. Sidorov, A. V. Palnichenko, and O. M. Vyaselev, "Superconductivity in Mg/MgO interface," *Physica C: Superconductivity*, vol. 480, pp. 123–125, Oct. 2012.

[4] E. A. Elkhalifa and H. B. Friedrich, "Magnesium oxide as a catalyst for the dehydrogenation of n-octane," *Arabian J. Chem.*, vol. 11, no. 7, pp. 1154–1159, Nov. 2018.

[5] N. M. Julkapli and S. Bagheri, "Magnesium oxide as a heterogeneous catalyst support," *Rev. Inorg. Chem.*, vol. 36, no. 1, pp. 1–41, 2015.

[6] R. R. Devi, I. M. Umlong, P. K. Raul, B. Das, S. Banerjee, and L. Singh, "Defluoridation of water using nano-magnesium oxide," *J. Experiment. Nano.*, vol. 9, no. 5, pp. 512–524, May 2014.

[7] X. Yang, L. Zhao, X. Li, and Y. Xiao, "Magnesium Oxide-Based Absorbents for CO$_2$ Capture at Medium Temperature," *Curr. Pollution Rep.*, vol. 4, no. 1, pp. 13–22, Mar. 2018.

[8] Y. Tolstova, S. T. Omelchenko, A. M. Shing, and H. A. Atwater, "Heteroepitaxial growth of Pt and Au thin films on MgO single crystals by bias-assisted sputtering," *Scientific Rep.*, vol. 6, p. 23232, Mar. 2016.

[9] P. P. Fedorov, E. A. Tkachenko, S. V. Kuznetsov, V. V. Voronov, and S. V. Lavrishchev, "Preparation of MgO nanoparticles," *Inorg. Mater.*, vol. 43, no. 5, pp. 502–504, May 2007.

[10] M. S. Mastuli, N. Kamarulzaman, M. A. Nawawi, A. M. Mahat, R. Rusdi, and N. Kamarudin, "Growth mechanisms of MgO nanocrystals via a sol-gel synthesis using different complexing agents," *Nanoscale Res. Lett.*, vol. 9, no. 1, p. 134, Mar. 2014.

[11] I. W. Sutapa, A. W. Wahab, P. Taba, and N. L. Nafie, "Synthesis and Structural Profile Analysis of the MgO Nanoparticles Produced Through the Sol-Gel Method Followed by Annealing Process," *Oriental J. Chem.*, vol. 34, no. 2, pp. 1016–1025, Apr. 2018.

[12] H. Cui, X. Wu, Y. Chen, and R. I. Boughton, "Synthesis and characterization of mesoporous MgO by template-free hydrothermal method," *Materials Resear. Bull.*, vol. 50, pp. 307–311, Feb. 2014.

[13] Z. Camtakan, S. (Akyil) Erenturk, and S. (Doyurum) Yusan, "Magnesium oxide nanoparticles: Preparation, characterization, and uranium sorption properties," *Environment. Prog. & Sustain.*, vol. 31, no. 4, pp. 536–543, 2012.

[14] K. V. Rao and C. S. Sunandana, "Structure and microstructure of combustion synthesized MgO nanoparticles and nanocrystalline MgO thin films synthesized by solution growth route," *J. Mater. Sci.*, vol. 43, no. 1, pp. 146–154, Jan. 2008.

[15] Z.-X. Tang and L.-E. Shi, "Preparation of nano-MgO using ultrasonic method and its characteristics," *Eclética Química*, vol. 33, no. 1, pp. 15–20, 2008.

[16] L.-Z. Pei, W.-Y. Yin, J.-F. Wang, J. Chen, C.-G. Fan, and Q.-F. Zhang, "Low temperature synthesis of magnesium oxide and spinel powders by a sol-gel process," *Mater. Research*, vol. 13, no. 3, pp. 339–343, Sep. 2010.

[17] M. Rezaei, M. Khajenoori, and B. Nematollahi, "Preparation of nanocrystalline MgO by surfactant assisted precipitation method," *Materials Resear. Bull.*, vol. 46, no. 10, pp. 1632–1637, Oct. 2011.

[18] R. Dobrucka, "Synthesis of MgO Nanoparticles Using Artemisia abrotanum Herba Extract and Their Antioxidant and Photocatalytic Properties," *Iran J. Sci. Technol. Trans. Sci.*, vol. 42, no. 2, pp. 547–555, Jun. 2018.

[19] M. S. Mastuli, N. Kamarulzaman, M. A. Nawawi, A. M. Mahat, R. Rusdi, and N. Kamarudin, "Growth mechanisms of MgO nanocrystals via a sol-gel synthesis using different complexing agents," *Nanoscale Res Lett*, vol. 9, no. 1, p. 134, Mar. 2014.

[20] M. C. D'Antonio, N. Mancilla, A. Wladimirsky, D. Palacios, A. C. González-Baró, and E. J. Baran, "Vibrational spectra of magnesium oxalates," *Vibrational Spectroscopy*, vol. 53, no. 2, pp. 218–221, Jul. 2010.

[21] F. Mohandes, F. Davar, and M. Salavati-Niasari, "Magnesium oxide nanocrystals via thermal decomposition of magnesium oxalate," *J. Phys. Chem. Solids*, vol. 71, no. 12, pp. 1623–1628, Dec. 2010.

[22] S. L. Reddy, T. R. Reddy, G. S. Reddy, T. Endo, and R. L. Frost, "Synthesis and spectroscopic characterization of magnesium oxalate nano-crystals," *Spectro. Acta Part A: Mol. Biomol. Spect.*, vol. 123, pp. 25–29, Apr. 2014.

[23] A. Kruk, "Fabrication of MgO high transparent ceramics by arc plasma synthesis," *Optical Mater.*, vol. 84, pp. 360–366, Oct. 2018.

[24] I. W. Sutapa, A. W. Wahab, P. Taba, and N. L. Nafie, "Dislocation, crystallite size distribution and lattice strain of magnesium oxide nanoparticles," *J. Phys.: Conf. Ser.*, vol. 979, p. 012021, Mar. 2018.

[25] Q. Zhu, A. R. Oganov, and A. O. Lyakhov, "Novel stable compounds in the Mg–O system under high pressure," *Phys. Chem. Chem. Phys.*, vol. 15, no. 20, pp. 7696–7700, May 2013.

[26] L. M. Loong *et al.*, "Strain-enhanced tunneling magnetoresistance in MgO magnetic tunnel junctions," *Scien. Reports*, vol. 4, p. 6505, Sep. 2014.

[27] M. J. L. Sangster, "Relaxations and their strain derivatives around impurity ions in MgO," *J. Phys. C: Solid State Phys.*, vol. 14, no. 21, pp. 2889–2898, Jul. 1981.

[28] S. Auzary, F. Badawi, L. Bimbault, J. Rabier, and R. J. Gaboriaud, "Stress and microstructure in YBaCuO thin films on MgO and SrTiO$_3$ substrates studied by X-ray diffraction and bending tests," *J. Alloys and Comp.*, vol. 251, no. 1, pp. 37–40, Apr. 1997.

[29] Y. Kawamura and H. Nakai, "Energy density analysis of embedded cluster models for an MgO crystal," *Chem. Phys. Lett.*, vol. 410, no. 1, pp. 64–69, Jul. 2005.

[30] R. Reali, F. Boioli, K. Gouriet, P. Carrez, B. Devincre, and P. Cordier, "Modeling plasticity of MgO by 2.5D dislocation dynamics simulations," *Mat. Sci. Enginer. : A*, vol. 690, pp. 52–61, Apr. 2017.

[31] M. Dongol, A. El-Denglawey, M. S. Abd El Sadek, and I. S. Yahia, "Thermal annealing effect on the structural and the optical properties of Nano CdTe films," *Optik*, vol. 126, no. 14, pp. 1352–1357, Jul. 2015.